JSE Journal of Systematics and Evolution

doi: 10.1111/jse.12560

Research Article

Plastome phylogenomic insights into the Sino-Japanese biogeography of *Diabelia* (Caprifoliaceae)

Hong-Xin Wang[1], Michael J. Moore[2], Russell L. Barrett[3], Sven Landrein[4], Shota Sakaguchi[5], Masayuki Maki[6], Jun Wen[7]*, and Hua-Feng Wang[1]*

[1]Key Laboratory of Tropical Biological Resources of Ministry of Education, School of Life and Pharmaceutical Sciences, Hainan University, Haikou 570228, China
[2]Department of Biology, Oberlin College, Oberlin, OH 44074, USA
[3]National Herbarium of New South Wales, Royal Botanic Gardens and Domain Trust, Sydney, NSW 2000, Australia
[4]Xishuangbanna Tropical Botanical Garden, Chinese Academy of Sciences, Menglun 666303, Yunnan, China
[5]Graduate School of Human and Environmental Studies, Kyoto University, Kyoto 606-8501, Japan
[6]Botanical Gardens, Tohoku University, Sendai 980-0862, Japan
[7]Department of Botany, Smithsonian Institution, Washington, DC 20013-7012, USA
*Authors for correspondence. Jun Wen. E-mail: wenj@si.edu; Hua-Feng Wang. E-mail: hfwang@hainanu.edu.cn
Received 30 August 2019; Accepted 22 December 2019; Article first published online 26 December 2019

Abstract Understanding the causes of the Sino-Japanese disjunctions in plant taxa has been a central question in eastern Asian biogeography, with vicariance or long-distance dispersal often invoked to explain such patterns. *Diabelia* Landrein (Caprifoliaceae; Linnaeoideae) comprises four shrubby species with a Sino-Japanese disjunct distribution. The species diversification time within *Diabelia*, covering a long geological history of the formation process of the Sino-Japanese flora, dated back to the middle Oligocene, therefore, *Diabelia* would be an ideal model to elucidate the biogeographic patterns of Sino-Japanese disjunctions with climate fluctuation. In this study, we analyzed complete plastome sequence data for 28 individuals representing all four species of *Diabelia*. These 28 plastomes were found to be highly similar in overall size (156 243–157 578 bp), structure, gene order, and content. Our phylogenomic analysis of the plastomes supported a close relationship between *Diabelia ionostachya* (Nakai) Landrein & R.L. Barrett var. *wenzhouensis* (S.L. Zhou ex Landrein) Landrein from eastern China and *Diabelia spathulata* (Siebold & Zucc.) Landrein var. *spathulata* from Japan. *Diabelia serrata* (Siebold & Zucc.) Landrein was identified as sister to a population of *Diabelia sanguinea* (Makino) Landrein from Tochigi in central Japan and *D. spathulata* Landrein, from Toyama, central Japan. Most *Diabelia* lineages were estimated to have differentiated 8–28 Mya. Our results indicate that two independent vicariance events could explain the disjunction between Japan and Korea in the mid to late Miocene, and between Zhejiang and Japan in the early Miocene.

Key words: biogeography, Caprifoliaceae, *Diabelia*, East Asia, phylogenetic relationship, plastome.

1 Introduction

Understanding the causes of intercontinental or regional disjunctions in plant taxa remains a central question in biogeography (e.g., Raven & Axelrod, 1974; Donoghue, 2008; Nie et al., 2012, 2013; Wen et al., 2013, 2016; Fritsch et al., 2015; Yi et al., 2015; Thomas et al., 2017). Disjunct distributions are usually explained by either vicariance or long-distance dispersal (Wiley, 1980; Doyle et al., 2004; Yoder & Nowak, 2006; Thomas et al., 2017; Harris et al., 2018; Yang et al., 2018). Vicariance occurs due to range contraction of a previously more widely distributed species and the fragmentation of the suitable habitat (Yoder & Nowak, 2006; Thomas et al., 2017), and can lead to reductions in gene flow that might ultimately lead to speciation (Nelson & Platnick, 1981; Humphries & Parenti, 1986). Long-distance dispersal events are typically mediated by wind, animals, or ocean currents (Carlquist,1996; Davis & Shaw, 2001; Xiang & Soltis, 2001; Cox & Moore, 2005; Dick et al., 2007; Gillespie et al., 2012; Appelhans et al., 2018; Price & Wagner, 2018; Zhao et al., 2018). A number of plant disjunctions have been reported to have resulted from long-distance dispersal, for example, in *Ampelopsis* Michaux and *Cyphostemma* (Planch.) Alston (Vitaceae) (Nie et al., 2012; Hearn et al., 2018), Loliinae (Poaceae) (Minaya et al., 2017), Loranthaceae (Liu et al., 2018), Sabiaceae (Yang et al., 2018), Urticeae (Urticaceae) (Huang et al., 2019), *Carex* L. (Cyperaceae) (Martín-Bravo et al., 2019), and Omphalodeae (Boraginaceae) (Otero et al., 2019).

During the Pleistocene interglacial periods, the Japanese archipelago underwent repeated separations from mainland Asia due to the submergence of a land bridge (Harrison et al., 2001).

These isolating events have resulted in vicariant distributions of numerous plant lineages between eastern China and Japan. For example, the distributions of *Cercidiphyllum* Siebold & Zucc. (Qi et al., 2012), *Kalopanax septemlobus* (Thunberg) Koidz. (Sakaguchi et al., 2012), *Platycrater arguta* Siebold & Zucc. (Qi et al., 2014), and *Neolitsea sericea* (Blume) Koidz. (Chen et al., 2015b) have all been influenced by fluctuations in the East China Sea. Despite progress, our understanding of the formation, phylogeography, and population genetics of the Sino-Japanese Floristic Region (SJFR) is still incomplete. Further studies on dispersal patterns of plant species distributed in the SJFR are required to determine the frequency of vicariance versus dispersal in this region, particularly with regard to the timing of biogeographic events (Qiu et al., 2011; Qi et al., 2012, 2014; Sakaguchi et al., 2017). Moreover, studies on groups of related species that occur in both Japan and China, rather than disjunct species or species pairs, are required. These studies would ideally use phylogenomic tools to supplement earlier studies based primarily on Sanger sequencing of traditional loci such as the nuclear internal transcribed spacer (ITS) and plastid loci (e.g., Allen et al., 2003; Mitsui et al., 2008; Qi et al., 2012, 2014; Sakaguchi et al., 2012; Kim et al., 2013; Cao et al., 2016; Niu et al., 2018).

Diabelia Landrein (Caprifoliaceae) represents an excellent opportunity to test plant speciation and phylogeography in the SJFR. This genus of shrubs was recently segregated from *Abelia* based on inflorescences of paired flowers appearing at the end of short shoots, and its separation is supported by DNA sequence data (Landrein, 2010; Wang et al., 2015, 2020; Zhao et al., 2019). Based on the number and length of sepals, Hara (1983) recognized three *Diabelia* species, with further distinctions made as varieties and forms based on hair types, nectary shape, fusion of nectaries and corolla, and corolla color. The three species are mainly distributed in Japan, with only a few populations in China and Korea (Hara, 1983; Zhou & Wen, 2006; Yang & Landrein, 2011; Shin et al., 2012; Zhao et al., 2019) (Fig. 1). One species, *Diabelia spathulata* (Siebold & Zucc.) Landrein is subdivided into three varieties (*D. spathulata* var. *spathulata*, var. *colorata* (H. Hara & S. Kuros.) Landrein and Landrein, which are distributed in southern, central, and northern areas of Japan (from Aomori to Saga prefectures) (Hara, 1983; Landrein & Farjon, 2020). Another species, *Diabelia serrata* (Siebold & Zucc.) Landrein is particularly variable and contains a number of infraspecific forms (*D. serrata* f. *serrata*, *D. serrata* f. *obspathulata* [Koidz.] Landrein, and *D. serrata* f. *tomentosa* [Koidz.] Landrein) that

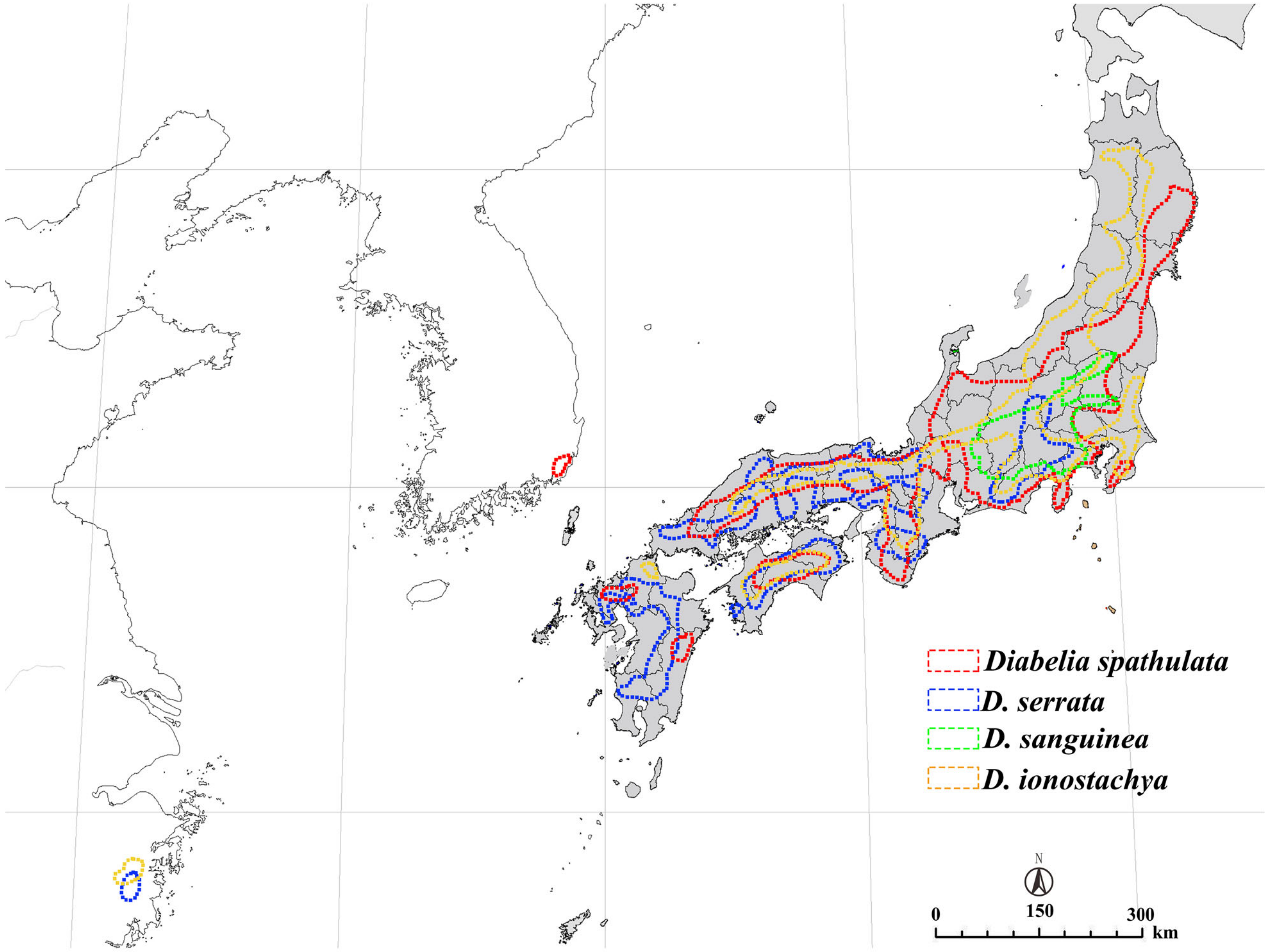

Fig. 1. Geographic distribution of each *Diabelia* species included in this study. The map is downloaded from http://library-muroran.opendata.arcgis.com/datasets.

are widely distributed in southern Japan, from Shiga to Kagoshima prefectures, as well as on the southeast coast of China (e.g., Sihaishan Mountain, Wenzhou, Zhejiang, Zhou & Wen, 2006). The other taxon, *Diabelia ionostachya* var. *tetrasepala* (Koidz.) Landrein is endemic to areas from Fukushima to Fukuoka prefectures in Japan, and its distribution overlaps with that of the other two taxa (*D. spathulata* and *D. serrata*) (Hara, 1983). Finally, based on the number of sepals, nectary cushion position, and corolla color, Landrein & Farjon (2020) have proposed the recognition of four species (e.g., *D. serrata*, *D. spathulata*, *D. sanguinea*, and *D. ionostachya* [Nakai] Landrein). Details of the distribution of these four species are shown in Fig. 1. However, there have been no explicit biogeographic analyses of the genus and it is unclear what role vicariance or potentially recent long-distance dispersal might have played in the biogeographic diversification of the genus in eastern Asia.

Previous molecular phylogenetic studies including *Diabelia* have not fully resolved the phylogenetic relationships among species and populations of *Diabelia*, and hence the biogeographic history of the genus remains poorly understood. In a study including four *Diabelia* species, five *Abelia* species, and three *Dipelta* species and using nuclear (ITS) and plastid sequence data, Landrein et al. (2012) found that *Abelia* is not monophyletic, and that *Kolkwitzia* Graebn., *Dipelta* Maxim., and *Diabelia* form a clade (bootstrap values = 82, posterior probabilities = 1.0). Using ITS2 and several plastid regions, Wang et al. (2015) resolved the same clade, with *Diabelia* sister to *Dipelta*. Zhao et al. (2019) found that *Diabelia* was divided into five gene pools: *D. serrata*, *D. spathulata*, *D. sanguinea*, *D. spathulata* var. *spathulata* in Korea, and *D. ionostachya* var. *ionostachya* in Yamagata Prefecture, northern Japan. However, these studies failed to resolve relationships within *Diabelia*, likely because the limited loci used failed to provide sufficient resolving power. Moreover, these studies did not include enough populations of *Diabelia* to fully explore the complex species-level relationships.

Complete plastome sequences provide many more informative sites for potentially greater phylogenetic resolution and support (Burke et al., 2012). The plastome is uniparentally inherited and has a highly conserved circular DNA arrangement (Park et al., 2018). Because of its relatively stable genome structure, gene content, and gene sequence, it is highly valuable and widely used in phylogenomic investigations (Wolfe et al., 1987; Raubeson & Jansen, 2005; Parks et al., 2009; Choi et al., 2016; Krak et al., 2016). Plastomes can provide valuable information for taxonomy and phylogenetic reconstruction of plants (Douglas, 1998; Huang et al., 2014). Complete plastome data have been used to resolve relationships at many taxonomic levels, including among closely related species, such as in Malpighiales (Xi et al., 2012), Arundinarieae (Poaceae) (Ma et al., 2014), *Euptelea* Sieb. & Zucc. (Eupteleaceae) (Cao et al., 2016), Arecaceae (Barrett et al., 2016), Vitaceae (Wen et al., 2018), “Asian Palmate” Araliaceae clade (Valcárcel & Wen, 2019), *Torreya* Arn. (Taxaceae) (Zhang et al., 2019), and Urticeae (Urticaceae) (Huang et al., 2019).

In this study, we leverage the power of complete plastomes to resolve relationships among the four species of *Diabelia* and investigate the biogeographic history of this Sino-Japanese genus. Here we report 28 new complete plastome sequences, covering all four species of *Diabelia*. Our objectives were to: (i) resolve the phylogenetic relationships among all *Diabelia* species and among closely related genera; (ii) investigate the biogeographic history of *Diabelia*; and (iii) characterize and compare the plastomes of *Diabelia*.

2 Material and Methods

2.1 Plant material and sampling design

We attempted to maximize the taxonomic and geographic coverage of *Diabelia* by using a broad sampling strategy. For convenience and uniformity, the samples used in our analysis were named according to the taxonomy proposed by Landrein & Farjon (2020). In total, 28 individuals were sampled. Fresh green leaves from adult plants of each species were collected in the field and immediately dried with silica gel for further DNA extraction. Voucher specimens were deposited in the Herbarium of the Institute of Tropical Agriculture and Forestry (HUTB), Hainan University (Haikou, China). Detailed information on the geographic distribution of the 28 samples and the localities in this study is shown in Table 1.

2.2 DNA extraction, plastome sequencing, assembly, and annotation

A modified CTAB protocol based on Doyle & Doyle (1987) was used to extract genomic DNA from dry leaf tissues. The genomic DNA of each sample was quantified and analyzed with an Agilent 2100 BioAnalyzer (UC Davis Genome Center, Davis, CA, USA). Samples yielding at least 0.8 μg DNA were selected for subsequent library construction and de novo sequencing. Genomic DNA of selected samples was used to build paired-end libraries with insert sizes of 200–400 bp. The complete plastomes of 28 accessions were sequenced using a BGISEQ-500 platform at BGI (Shenzhen, China), yielding approximately 8 Gb of high-quality sequences per sample of 100 bp paired-end reads. Raw reads were filtered and trimmed using SOAPfilter_v2.2 to exclude reads with >10% Ns, reads with >40% low quality bases (quality scores ≤10), and reads contaminated by adaptors and/or produced by PCR duplication. Approximately 6 Gb of clean data was obtained from each individual and was assembled against the plastomes of a closely related genus (*Kolkwitzia amabilis* Graebn.; GenBank accession No. NC_029874.1 (Bai et al., 2017)) using MITObim version 1.8 (Hahn et al., 2013). Plastomes were annotated with Geneious R8.0.2 (Biomatters, Auckland, New Zealand) and DOGMA (Wyman et al., 2004). Maps of the *Diabelia* plastomes were created using Organellar Genome DRAW (OGDRAW; Lohse et al., 2013), with subsequent manual editing.

2.3 Plastome sequence divergence analysis and molecular marker identification

Alignments of the 28 *Diabelia* complete plastome sequences were visualized using mVISTA. Default parameters were utilized to align the chloroplast genomes in Shuffle-LAGAN mode and a sequence conservation profile was visualized in an mVISTA plot (Frazer et al., 2004). We extracted all the

Table 1 Summary of major characteristics of *Diabelia* plastomes, including aspects of plastome size, G-C content, and gene number, collection site, and voucher specimen number

Species	General collection site	Voucher specimen No.	Plastome size (bp)	LSC length (bp)	SSC length (bp)	IR length (bp)	Total GC (%)	LSC (%)	SSC (%)	IR (%)	Protein coding	tRNA genes	rRNA genes	GenBank accession No.
D. ionostachya var. *wenzhouensis*	Wenzhou, China	HUTB, cp5701	156 942	90 264	18 930	23 874	38.4	36.50	32.90	44.20	79	30	4	MK033526
D. serrata	Shimane, Japan	HUTB, e0310	156 755	89 910	18 857	23 ,937	38.5	36.60	33.10	44.20	79	30	4	MK033527
D. serrata	Shiga, Japan	HUTB, e1301	157 136	90 230	18 892	24 007	38.5	38.50	33.10	44.30	79	30	4	MK033528
D. serrata	Fukui, Japan	HUTB, e2901	157 021	90 095	18 870	24 028	38.5	36.60	33.20	44.30	79	30	4	MK033529
D. serrata	Gifu, Japan	HUTB, e3401	156 500	89 937	18 885	23 839	38.5	36.60	33.10	44.30	79	30	4	MK033530
D. serrata	Tokushima, Japan	HUTB, e3616	156 738	89 980	18 886	23 936	38.5	36.60	33.10	44.20	79	30	4	MK033531
D. serrata	Tokushima, Japan	HUTB, e3703	156 676	90 014	18 820	23 921	38.5	36.60	33.10	44.20	79	30	4	MK033532
D. serrata f. *buchwaldii*	Ehime, Japan	HUTB, e5202	156 551	89 802	18 869	23 940	38.5	36.60	33.10	44.20	79	30	4	MK033541
D. serrata f. *tomentosa*	Kochi, Japan	HUTB, e5801	156 747	89 976	18 915	23 928	38.5	36.60	33.10	44.20	79	30	4	MK033542
D. ionostachya var. *ionostachya*	Yamagata, Japan	HUTB, p2017	156 856	90 115	18 959	23 891	38.4	36.50	33	44.20	79	30	4	MK033543
D. sanguinea	Tochigi, Japan	HUTB, p2102	156 842	90 102	18 894	23 923	38.5	36.60	33.20	44.20	79	30	4	MK033544
D. spathulata	Toyama, Japan	HUTB, p2406	157 012	90 205	18 889	23 959	38.5	36.60	33.20	44.10	79	30	4	MK033545
D. spathulata var. *spathulata*	Aichi, Japan	HUTB, p2603	156 637	89 868	18 911	23 929	38.4	36.50	33	44.20	79	30	4	MK033546
D. serrata	Tokushima, Japan	HUTB, e3704	156 614	89 949	18 885	23 890	38.5	36.60	33.10	44.20	79	30	4	MK033533
D. serrata	Tokushima, Japan	HUTB, e3715	157 089	90 347	18 904	23 919	38.4	36.50	33.10	44.10	79	30	4	MK033534
D. serrata	Tokushima, Japan	HUTB, e4202	157 169	90 361	18 930	23 939	38.4	36.50	33.10	44.20	79	30	4	MK033535
D. serrata	Tokushima, Japan	HUTB, e4226	156 835	90 175	18 872	23 894	38.5	36.50	33.10	44.20	79	30	4	MK033536
D. serrata	Tokushima, Japan	HUTB, e4813	157 452	90 573	18 943	23 968	38.4	36.50	33.10	44.20	79	30	4	MK033537
D. serrata f. *buchwaldii*	Kochi, Japan	HUTB, e5018	157 578	90 559	18 951	24 034	38.5	36.60	33.10	44.20	79	30	4	MK033538
D. serrata	Kochi, Japan	HUTB, e5101	157 176	90 345	18 885	23 973	38.5	36.60	33.10	44.20	79	30	4	MK033539
D. serrata	Kochi, Japan	HUTB, e5115	156 243	89 539	18 818	23 943	38.6	36.60	33.20	44.20	79	30	4	MK033540
D. spathulata var. *spathulata*	Kochi, Japan	HUTB, p6102	156 733	89 928	18 869	23 968	38.5	36.50	33.10	44.30	79	30	4	MK033551

Continued

Table 1 Continued

Species	General collection site	Voucher specimen No.	Plastome size (bp)	LSC length (bp)	SSC length (bp)	IR length (bp)	Total GC (%)	LSC (%)	SSC (%)	IR (%)	Protein coding	tRNA genes	rRNA genes	GenBank accession No.
D. spathulata var. *spathulata*	Korea	HUTB, p5601	157 561	90 801	19 072	23 774	38.4	36.50	33	44.20	79	30	4	MK033549
D. serrata	Tokushima, Japan	HUTB, t3205	156 874	90 244	19 042	23 726	38.5	36.50	33.10	44.30	79	30	4	MK033552
D. serrata	Tokushima, Japan	HUTB, t3209	156 635	89 947	18 820	23 934	38.5	36.60	33.20	44.10	79	30	4	MK033553
D. spathulata var. *spathulata*	Nara, Japan	HUTB, p2701	157 127	90 275	18 872	23 990	38.4	36.50	33	44.20	79	30	4	MK033547
D. spathulata var. *spathulata*	Ehime, Japan	HUTB, p2801	156 810	90 051	18 863	23 948	38.4	36.50	33	44.20	79	30	4	MK033548
D. spathulata var. *spathulata*	Kochi, Japan	HUTB, p6101	157 144	90 331	18 887	23 963	38.4	36.50	33.10	44.20	79	30	4	MK033550

IR, inverted repeat (A or B) regions; LSC, large single-copy region; rRNA, ribosomal RNA; SSC, small single-copy region; tRNA, transfer RNA.

coding regions, introns, and intergenic spacers under the following two criteria: (i) total number of mutations (Eta) >0; and (ii) an aligned length >200 bp to explore the divergence hotspot regions in *Diabelia* and facilitate its utilization in identification. For identifying hypervariable regions, nucleotide diversity (*Pi*) for all protein-coding and non-coding (intergenic spacer and intron) regions was calculated from the sequence alignment of all 28 complete *Diabelia* plastomes using a sliding window analysis in DnaSP version 5.10 (Librado & Rozas, 2009).

2.4 Phylogenetic analyses

Phylogenetic analyses of *Diabelia* were carried out using both maximum likelihood (ML) and Bayesian inference (BI) methods based on an alignment of 28 complete plastomes (excluding one copy of the inverted repeat (IR)) of *Diabelia* and four outgroup sequences (two of *Dipelta floribunda* Maxim., *Dipelta yunnanensis* Franch, and *K. amabilis*). Seven main concatenated datasets were assembled for phylogenetic analyses: large single copy (LSC) region, small single copy (SSC) region, IR region, complete plastome, all protein coding genes, all non-coding regions, and complete plastomes minus one copy of the IR region.

The alignments were constructed using MAFFT version 7 (Katoh & Standley, 2013). The evolutionary model (best-fit) was most appropriate for all the data according to the corrected Akaike Information Criterion implemented in jModelTest version 2.1.7 (Santorum et al., 2014). The ML analysis was carried out using RAxML-HPC version 8.2.20 (Stamatakis, 2014) using the default parameters and 1000 bootstrap replicates. The BI analysis was undertaken using MrBayes version 3.2 (Huelsenbeck & Ronquist, 2001), with two independent Markov chain Monte Carlo (MCMC) runs, a random starting tree, and default priors for 5 000 000 generations, with trees sampled every 1000 generations. Convergence of the MCMC chains was assumed when the average standard deviation of split frequencies reached 0.01 or less. Both analyses were undertaken on the CIPRES Science Gateway website (Miller et al., 2010). FigTree version 1.3.1 (Drummond et al., 2012) was used to visualize the resulting phylogenetic trees.

2.5 Divergence time estimation

Molecular dating analyses using the complete plastome (excluding one copy of the IR) DNA dataset were undertaken in BEAST using a GTR + G substitution model (as selected by MrModelTest (Posada, 2008)) and an uncorrelated lognormal relaxed clock (Drummond et al., 2002). A Yule process was specified as the tree prior. Two calibration points were used to constrain each node. A fruit fossil of the genus *Diplodipelta* from the late Eocene Florissant flora of Colorado (34.07 Ma; Manchester, 2001) was considered to be the oldest possible date for the age of *Dipelta*. Hence, we set the stem of *Dipelta* with a lognormal mean = 0, SD = 1.0, and an offset = 34.07 Ma. In addition, a secondary calibration point based on the crown age of *Kolkwitzia*, *Diabelia*, and *Dipelta* as recovered in the analysis of Wang et al. (2015) (40.18 Ma, 95% highest posterior density (HPD): 36.85–44.68 Ma) was used to constrain the *Kolkwitzia*, *Diabelia*, and *Dipelta* crown node to 40.18 Ma, with a normal prior, mean = 40.18 Ma, SD = 2. The analyses were run for

30 000 000 generations with parameters sampled every 5000 generations. The effective sample size (>200) was determined using Tracer version 1.6 (Drummond et al., 2012) and the first 10% of the samples were discarded as burn-in. Tree Annotator version 1.8.0 (Drummond et al., 2012) was used to summarize the set of post-burn-in trees and their parameters in order to produce a maximum clade credibility chronogram showing the mean divergence time estimates with 95% HPD intervals. FigTree version 1.3.1 (Drummond et al., 2012) was used to visualize the resulting divergence times.

2.6 Ancestral area reconstructions

Statistical Dispersal-Vicariance Analysis (S-DIVA) was applied to infer ancestral areas of *Diabelia*. This tool reconstructs the ancestral distribution at each of the internal nodes of a given phylogeny. This is accomplished by means of optimization rules and set costs for extinction (cost of one per area lost) and dispersal (cost of one per area added). Vicariance and sympatric speciation carry no cost (Ronquist, 1997; Nylander et al., 2008; Velazco & Patterson, 2008; Harris & Xiang, 2009; Yu et al., 2010, 2019). To reconstruct the geographic diversification of *Diabelia*, S-DIVA analysis as implemented in RASP (version 4.0; Yu et al., 2015, 2019) was carried out.

All taxa in this study were assigned to two of the biogeographic areas proposed by Hara (1983) and Yang & Landrein (2011), with additional division of the Japanese mainland. Specifically, the following five areas were defined to cover the present distributional ranges of the four *Diabelia* species and their close relatives (e.g., *Dip. yunnanensis* and *K. amabilis*): (A) Japan archipelago; (B) Korea; (C) southeast China (Wenzhou in Zhejiang province); (D) northwest China (e.g., Shaanxi, Shanxi, Hubei provinces); and (E) southwest China (e.g., Yunnan province) (Table 1). The biogeographic changes in S-DIVA reconstructions are assumed to occur along branches and not at the nodes of the phylogeny. The maximum number of areas observed for any terminal is one, and S-DIVA requires at least two areas (i.e., the possibility of wider ancestral ranges). Therefore, we constrained the ancestral distribution to include a maximum of two areas. Ancestral reconstructions are averaged over all trees in a Bayesian sample to account for phylogenetic uncertainty in the biogeographic analysis; therefore, 20 000 trees from the BEAST MCMC outputs were used, and the BEAST annotated tree was set as the final condensed tree. The other parameters were automatically optimized.

3 Results

3.1 Genome structure, gene content, and divergent sequence hotspot regions

All 28 newly sequenced plastomes were completely assembled and their structures were very similar (Figs. S1A, S1B). Among all *Diabelia* plastomes, the length ranged from 156 243 to 157 578 bp (Fig. 2; Table 1). The plastomes were composed of an LSC region (89 539–90 801 bp), SSC region (18 818–19 072 bp), and two IR copies (23 726–24 034 bp) (Fig. 2; Table 1). Their overall G/C content ranged from 32.9% to 44.3%. The 28 plastomes encoded 124 genes, including 79 protein-coding genes, 37 tRNA genes, and eight rRNA genes. Within the IR, eight tRNA genes, seven protein-coding genes, and all four rRNA genes were completely duplicated. Sequence identity was found to be 98% among all *Diabelia* plastomes; the mVISTA alignment of all *Diabelia* plastomes is shown in Fig. S1C. The regions with the highest amount of divergence were distributed in intergenic spacers (Fig. S1C; Table S1). In total, 211 loci (81 coding genes and 130 non-coding regions) were compared for *Diabelia*, and *Pi* values ranged from 0.0 (e.g., *rpoC1-rpoB* [parsimony informative characters, PIC = 0]) to 0.0496 (*ndhF-rpl32*, PIC = 11) (Fig. S1C; Table S1). The mean value of *Pi* in non-coding regions was 0.0073, which was almost three times as much as in the coding regions. Intergenic spacer regions with *Pi* > 0.03 were *ndhF-rpl32, trnR-UCU-atpA, trnH-GUG-ycf2, trnH-GUG-psbA, rrn5-trnR-ACG, clpP-psbB, psaJ-rpl33, and rps12-clpP.*

3.2 Phylogenetic analyses

Both ML and BI methods produced mostly congruent topologies across different datasets (e.g., LSC, SSC, and IR) and partitioning strategies (Figs. 3, S2I–2VI). All samples of *D. serrata* formed a monophyletic group, here designated as SE. The three samples of *D. ionostachya* did not form a clade, and these were designated as DI1 and DI2. *Diabelia spathulata* formed two clades, SP1 and SP2. As only one accession of *D. sanguinea* was included, we designated it as SA. All of our datasets except the IR region, coding region, and non-coding regions suggested that samples of *D. serrata* formed a clade (Figs. 3, S2I–2VI; Table S2).

3.3 Divergence time estimation

The BEAST-derived chronogram also recovered *Diabelia* as monophyletic (Fig. 4), with an estimated crown age of ca. 28.27 Ma (95% HPD, 22.95–33.90 Ma), followed by the divergence of *Diabelia* into two lineages, for example, southwest Japan–east China (Zhejiang) and northeast–central Japan. The crown age of *D. spathulata* from southwest Japan (Nara, Ehime, Aichi, Kochi) to east China (Zhejiang) was predicted to be 20.67 Ma (95% HPD, 13.11–27.73 Ma), which is also the divergence time of Chinese *D. ionostachya* and Japanese *D. spathulata*.

The estimated crown age of *D. serrata*, *D. sanguinea* (+ *D. spathulata*), and *D. ionostachya* from Yamagata (+ *D. ionostachya from* Korea) was 26.18 Ma (95% HPD, 20.11–30.15 Ma), whereas the crown age of *D. serrata* and *D. sanguinea* (+ *D. spathulata*) was 19.13 Ma (95% HPD, 14.57–24.98 Ma). The crown age of *D. ionostachya* var. *ionostachya* Yamagata and *D. spathulata* var. *spathulata* from Korea was 9.02 Ma (95% HPD, 3.13–16.30 Ma). In addition, most of the lineages of *Diabelia* differentiated from 8 to 28 Ma (early Oligocene–late Miocene).

3.4 Ancestral area reconstruction

The results of the reconstruction of ancestral geographic distribution are shown in Fig. 5. Our analyses revealed two dispersal events and two vicariance events among the three defined biogeographic areas (Fig. 5). The ancestor of *Diabelia* was inferred to have been present throughout region A during the early Miocene (Fig. 5), with subsequent dispersal or vicariance across Japan, Korea, and China. The results indicate a Japanese archipelago origin for the genus *Diabelia* during the Eocene/Oligocene boundary. *Diabelia ionostachya* from Korea was also suggested to have originated in

Fig. 2. Comparison of large single copy (LSC), inverted repeat (IR), and small single copy (SSC) junction positions among the 28 *Diabelia* plastomes.

northwest Japan. However, one vicariance event was detected on node II, which indicates gene flow from regions A and C.

4 Discussion

4.1 Phylogenetic relationships

In our analyses, of the four species of *Diabelia* only *Diabelia serrata* was recovered as monophyletic (only one sample of *D. sanguinea* was included; Fig. 3). Both *D. spathulata* and *D. ionostachya* were non-monophyletic (Fig. 3). Similarly, Zhao et al. (2019) also failed to recover species monophyly in plastid data in *Diabelia*. Each of the two species recovered as non-monophyletic in our analyses is coherent morphologically. For example, Hara (1983) pointed out that the nectary of *D. ionostachya* is distinct because it is flat and remains fused to the corolla, whereas the nectary is free in *D. spathulata*. Landrein & Farjon (2020) also identified similarities among *D. ionostachya* var. *ionostachya*, *D. ionostachya* var. *tetrasepala*, and *D. ionostachya* var. *wenzhouensis*, including flower size and the shape of the nectary (although the nectary of var. *wenzhouensis* has so far not been observed). Likewise, Hara (1983) identified the presence of five sepals as the main morphological character that defines *D. spathulata*. Based on corolla size and nectary structure, Landrein et al. (2017) recircumscribed the species by separating out *D. ionostachya* from *D. spathulata* based on the former having a nectary cushion that is clavate and apically free from the corolla tube versus a cushion that is fused to the corolla tube. The separation of *D. spathulata* could also signal that it should be raised to specific status. However, without additional nuclear data, it is premature to make such changes. Nevertheless, if future analyses support the non-monophyly of the currently accepted *Diabelia* species, it suggests that some morphological character states used in the current taxonomy of the genus might have had multiple origins or be plesiomorphic.

The non-monophyly of *D. spathulata* and *D. ionostachya* in our analyses could have resulted from gene flow (hybridization–introgression) or from multiple origins of these morphotypes. It is possible that some of this

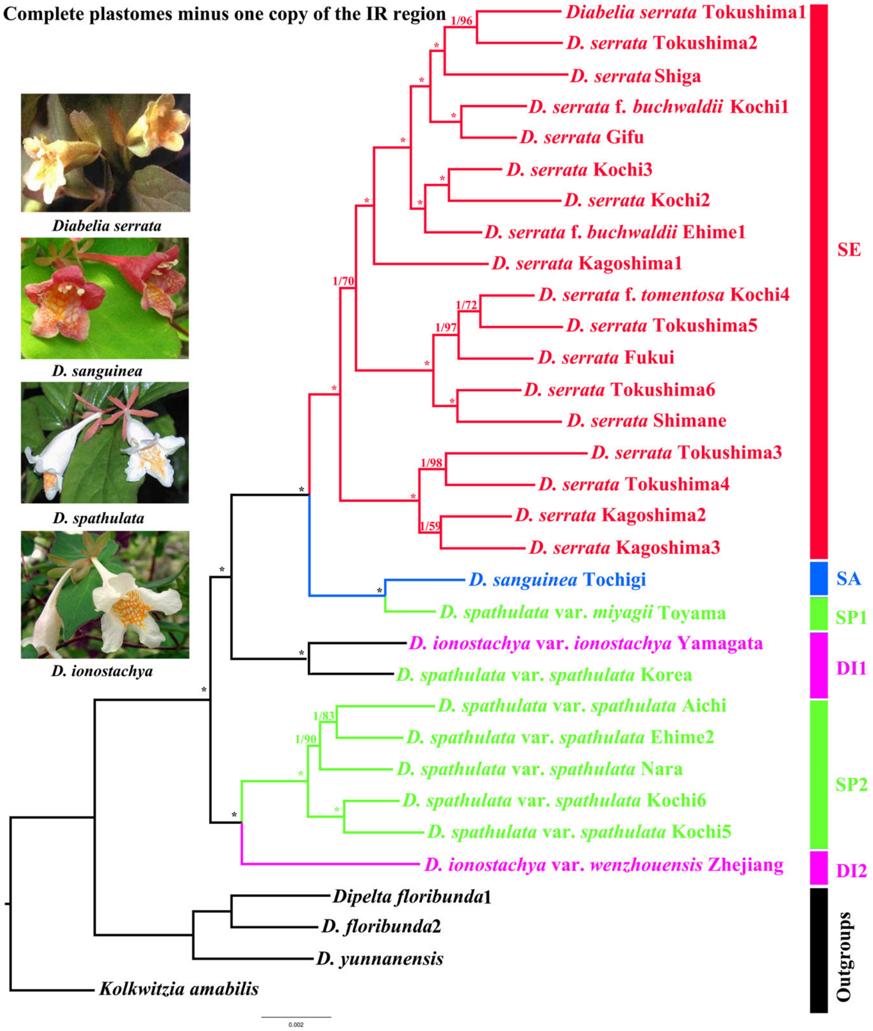

Fig. 3. Phylogenetic relationships of *Diabelia* inferred from maximum likelihood (ML) and Bayesian inference (BI), based on 28 complete plastomes (excluding one copy of the inverted repeat (IR)). Support values marked above the branches follow the order posterior probability (PP)/maximum parsimony bootstrap support (BS). Asterisks represent nodes with maximal support values in all analyses.

non-monophyly could be due to chloroplast capture events or incomplete lineage sorting during the speciation process, as reported in other studies (e.g., Yuan & Olmstead, 2008; Acosta & Premoli, 2010; Wang et al., 2013b; Yi et al., 2015; Kawabe et al., 2018). However, given the low resolution of the nuclear data for *Diabelia* it is difficult to distinguish among chloroplast capture versus true polyphyly.

Given that the current overlap of *Diabelia* species is considerable for each species, recurrent dispersal from ice age refugia (probably scattered along the Pacific coast of Japan for these thermoplastic shrubs) and secondary contacts could have taken place repeatedly. In addition, the plastome is a haploid, uniparentally inherited, single locus (Birky, 1995; Feng et al., 2019). Comparative phylogenies and phylogeography between biparental (nuclear) and uniparental (chloroplast) markers are needed to elucidate the timing and processes underlying species diversification, hybridization, and range evolution within *Diabelia* (Qi et al., 2012; Lu et al., 2017, Niu et al., 2018). In the future, multilocus phylogenies, phylogeographic studies, and paleoclimatic niche modeling are required to explore the time scales and demography of species divergences as well as hybridization in this genus.

4.2 On the differentiation of *Diabelia* species

At present, many phylogeographic and population genetics studies have been undertaken in the SJFR (e.g., Qiu et al., 2011; Qi et al., 2012, 2014; Chen et al., 2015b; Sakaguchi et al., 2017). However, few studies have examined geographically uneven distribution patterns such as that seen in *Diabelia*, especially those that involve taxa that are narrowly distributed in China and Korea but widely distributed in Japan. Furthermore, most studies have focused only on varieties or subspecies of a single species or a related species pair (e.g., Qiu et al., 2011; Qi et al., 2012, 2014; Chen

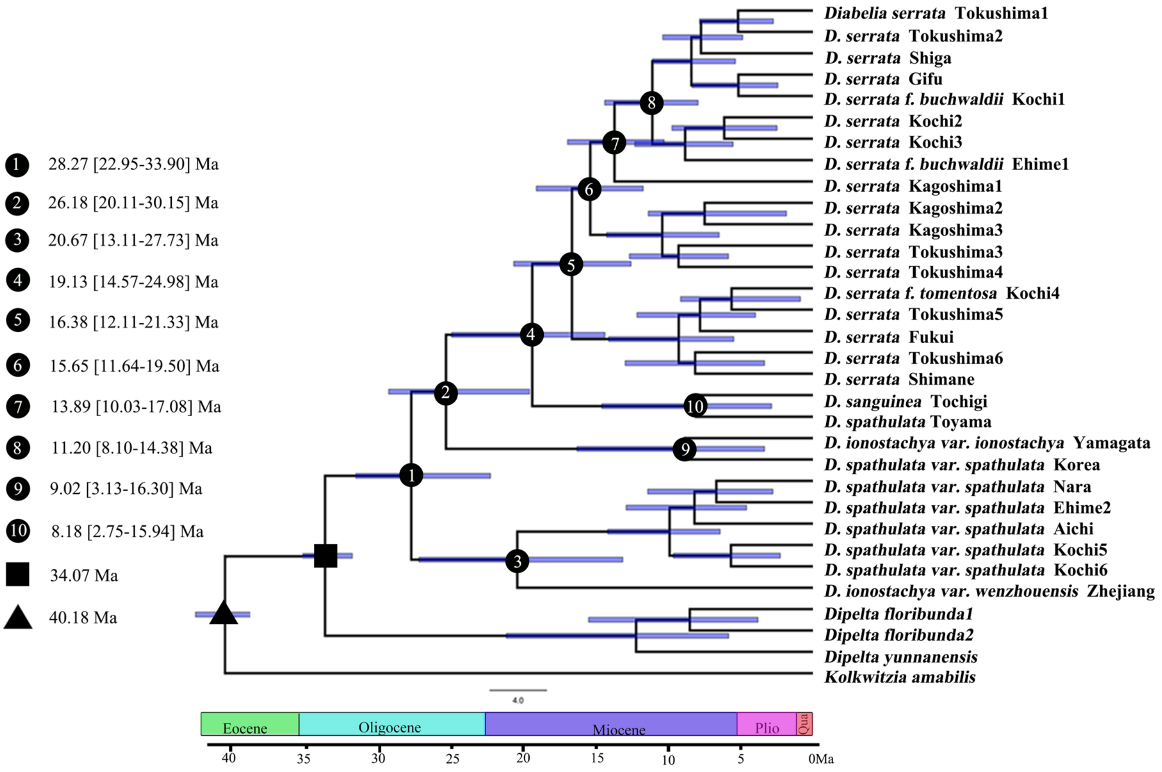

Fig. 4. Beast chronogram of *Diabelia* and outgroups based on complete plastome (excluding one copy of the inverted repeat) sequence data. Calibration points are indicated by triangles or squares. Blue bars on nodes indicate average ages of nodes with 95% highest posterior density.

et al., 2015a; Sakaguchi et al., 2017). In this study, we included all species of *Diabelia*, using the genus as a model to explore the origin and formation of the Sino-Japanese flora.

4.2.1 Potential demographic stability of *D. ionostachya* var. *wenzhouensis*

In contrast to the profound influence of the Quaternary climatic fluctuations on the range dynamics of both *Cercidiphyllum japonicum* Sieb. & Zucc. (Qi et al., 2012) and *Sargentodoxa cuneata* (Oliv.) Rehd. et Wils. (Tian et al., 2015) in China, our results suggest that the lineage leading to *D. ionostachya* var. *wenzhouensis* diverged in the early Miocene (Fig. 4). *Diabelia ionostachya* var. *wenzhouensis* is mainly distributed in a narrow region of Mount Sihaishan of Zhejiang in eastern China (Zhou & Wen, 2006). Our analyses recovered a divergence time of 20.67 Ma (95% HPD, 13.11–27.73 Ma; Fig. 4) between this species and its sister clade, suggesting a potentially long period of habitation in China for this lineage. Conversely, it is not possible to rule out a more recent dispersal event to explain the localized distribution of var. *wenzhouensis*, because we were able to include only one individual. Confirming the phylogenetic position of var. *wenzhouensis* will require more nuclear data (Zhao et al., 2019). Nevertheless, the potential long-term persistence of this population might have been facilitated by periodic episodes of up-slope contraction during interglacials, and down-slope expansion during glacials, with populations tracking favorable humidity conditions as imposed by the East Asian monsoon in areas of high relief. If *Diabelia ionostachya* var. *ionostachya* and *D. ionostachya* var. *wenzhouensis* are truly distinct species, their similarity in reproductive morphology could be due to coevolution of pollinators or fruit dispersal mechanisms.

4.2.2 Rapid differentiation of *D. serrata*

Zhao et al. (2019) suggest that *D. serrata* is composed of two phylogroups with unique sets of plastid haplotypes and distinct geographic distributions, one in Japan (central and south Japan) and the other in Zhejiang, China (fig. 2 from Zhao et al., 2019). The presence of only two sepals has been considered as the most reliable morphological character to identify *D. serrata* (see Hara, 1983). However, its morphology is more variable than previously considered, as the sepal number varies from 2 to 4. In addition, the flowers are paired or sometimes in clusters of 4–7 flowers, the corolla is 9–22 mm long, and the corolla color varies from yellow to light yellow, white, or red (Landrein & Farjon, 2020). Our molecular dating analyses (see Fig. 4) indicate that the onset of diversification in *D. serrata* occurred during the mid to late Miocene. This species is widely distributed in Japan and sporadically distributed in China, so we speculate that it arrived there by long-distance dispersal from Japan.

4.3 Biogeographic diversification of *Diabelia* in the Sino-Japanese floristic region

The eastern edge of the Sino-Japanese region, ranging from southeast China to mainland Japan and the Korean

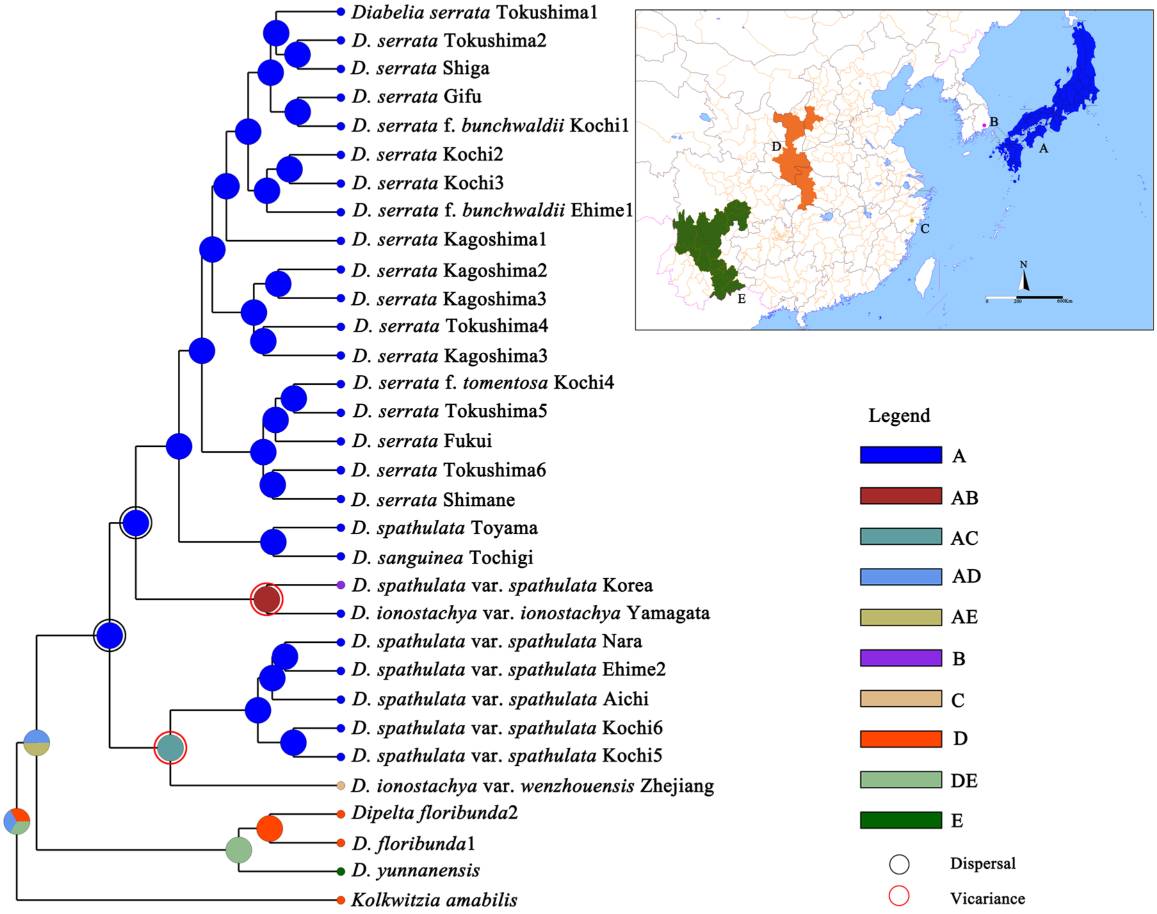

Fig. 5. Ancestral area reconstruction for *Diabelia*. Ancestral area reconstructions based on the Statistical Dispersal-Vicariance Analysis (S-DIVA) method implemented in RASP, using the BEAST-derived chronogram of *Diabelia.* The map at upper right shows major distribution regions of *Diabelia* included in the S-DIVA analysis: (**A**) Japan archipelago; (**B**) Korea; (**C**) southeast China (Wenzhou, Zhejiang); (**D**) northwest China (e.g., Shaanxi, Shanxi, Hubei); (**E**) southwest China (e.g., Yunnan). **D** and **E** are the outgroups. Pie charts at each node illustrate the marginal probabilities for each alternative ancestral area derived from S-DIVA, with the maximum area number set to two. The map is downloaded from https://zhfw.tianditu.gov.cn/.

Peninsula, is included in the Sino-Japanese Forest subkingdom. This region is also characterized by a remarkably rich flora and high rainfall due to the southeastern monsoon (Takhtajan, 1969, 1986; Wen, 1999; Harrison et al., 2001; Qiu et al., 2011). The *Diabelia* species in this region could have evolved allopatrically due to the topogeographical variation due to fluctuations in sea level during the Miocene (Fig. 5). It is generally known that many species show disjunctive distributions (e.g., *Kalopanax septemlobus*, Sakaguchi et al., 2012; *Neolitsea sericea*, Chen et al., 2015b), whether due to long-distance dispersal or vicariance, or from a combination of both. Under a hypothesis of long-distance dispersal, it would be predicted that a lineage in one region should nest within a lineage from a separate, disjunctive region. In contrast, under vicariance, lineages from different geographic regions would be monophyletic, with relatively comparable levels of genetic diversity in each of the regions of distribution (Yoder & Nowak, 2006; Liao et al., 2016; Thomas et al., 2017).

Our molecular dating indicated that *Diabelia* originated in the Japanese archipelago (region A; Fig. 5) and that species in the genus differentiated 8–28 Ma ago (Fig. 4), which is after the isolation of the Japanese islands. The Japanese archipelago originated as a direct extension of the Asian continent during the Tertiary and formed part of the Asian continent until at least the early Miocene (Hotta, 1974; Iijima & Tada, 1990; Li et al., 1996; Maekawa, 1998). After the separation of Japan from the Asian mainland, land connections formed between Japanese islands and the Asian mainland periodically during the Miocene (7.0–5.0 Ma) and Quaternary (2.0–1.3 Ma, 0.2–0.015 Ma), likely playing an important role in plant migrations (Harrison et al., 2001). Climate shifts in the mid to late Tertiary resulted in the rise and fall of the East China Sea levels, providing opportunities for the expansion, contraction, and isolation of *Diabelia* in East Asia, which might have also led to the deeper divergences within *Diabelia* (Qian & Ricklefs, 2000; Qi et al., 2012; Zhai et al., 2012; Sakaguchi et al., 2017; Zhao et al., 2019). Successful colonization after long-distance dispersal depends on the availability and competitiveness of suitable habitats (Minaya et al., 2017). It is remarkable that all *Diabelia* species have fruit-forming samaras (Landrein, 2010), increasing long-distance dispersal abilities relative to allied genera with non-winged propagules. *Diabelia ionostachya* in Yamagata and *D. spathulata* in Korea diverged in the late Miocene, at approximately 9.02 Ma (95% HPD, 3.13–16.30 Ma). Furthermore, our data suggest that the population of *D. spathulata* in Korea has a long evolutionary history, possibly dating back to the mid to late Miocene (node I, Fig. 5). It is well-known that the global temperatures began to drop significantly from the mid-Miocene onwards (Zachos et al., 2001). When the temperature fell, glacial refuges might have been formed in the southern part of the Korean Peninsula (Qiu et al., 2009, 2011). The vicariant event of the Korean *D. spathulata* in the mid to late Miocene (Fig. 5) represents a good example of the Korean–Japan Miocene connection.

4.4 Influence of climate change on *Diabelia* distribution

In general, species distributions during the Quaternary were greatly affected by glacial and interglacial fluctuations (Comes & Kadereit, 1998; Hewitt, 2000), and this is likely to have been the case in *Diabelia* as well. Most plant distributions underwent expansion and contraction, leading to population migration or extinction, followed by geographic isolation, differentiation, and subsequent population expansion (e.g., Li et al., 2008; Wang et al., 2013a). Our divergence time estimates suggest that the crown group of *Diabelia* originated in the late Oligocene (28.27 Ma; 95% HPD, 22.95–32.90 Ma), suggesting that extant populations likely differentiated well before the Last Glacial Maximum (LGM, ca. 18 000 years ago), similar to the findings of Wang et al. (2015). Reconstructions of the past vegetation of East Asia based on palynological data (Harrison et al., 2001) suggest that during the LGM and possibly during earlier cold periods as well, the extant range of *Diabelia* in east China and south Japan was covered by mixed (temperate and boreal) forest at higher elevations and warm temperate deciduous forest at lower elevations, with the latter broadly extending across the land bridge of the exposed East China Sea. During that time, warm temperate evergreen forest was forced to retreat southward as far as 24°N on the Asiatic mainland (Yu et al., 2000; Harrison et al., 2001), or, in Japan, survived in narrow glacial refuges on the Pacific Ocean side (Kamei et al., 1981; Dobson, 1994). In our studies, the potential range for *Diabelia* species in mainland China would have been much smaller, while habitats would have remained stable across most of the current distribution area within Japan. According to Qian (2002), the temperate forests extended across the continental shelf, connecting the populations in China, Korea, and Japan during the LGM, while the high sea levels during interglacial periods separated these regions. Our divergence time analysis (Fig. 4) suggested that the population of *D. ionostachya* from Zhejiang diverged in the early Miocene, at approximately 20.67 Ma (95% HPD, 13.11–27.73 Ma). Our results suggest a vicariance event associated with *D. ionostachya* in Zhejiang (Fig. 5). All *Diabelia* species analyzed in this study are shrubs with potentially long-distance dispersal abilities. Considering this, it is likely that dispersal should have been frequent enough to ensure rapid range expansions following glacial retreat. The range expansions could have begun from populations in different refugia. Hence, the disjunction between *D. ionostachya* in Zhejiang and *D. spathulata* in Japan might also have resulted from migration across this land bridge followed by vicariance. Nevertheless, we cannot rule out direct long-distance dispersal between Japan and Korea. Similar patterns between China and Japan have been documented in many studies (e.g., *Cercidiphyllum japonicum* (Qi et al., 2012), *Euptelea* (Cao et al., 2016)). This study adds another example of this well-documented pattern.

The distribution of each current species pair within *Diabelia* greatly overlaps (Fig. 1). Recurrent dispersal from ice age refugia (probably scattered along the Pacific coast for these thermoplastic shrubs) and secondary contacts might have taken place repeatedly (Qi et al., 2012, 2014; Chen et al., 2015b). These events could have blurred the biogeographic signals within the Japanese islands, which might have been generated during times when the lineages were geographically isolated (Sakaguchi et al., 2012). Although Zhao et al. (2019) assessed the influence of introgression in shaping species boundaries in the Japanese archipelago using chloroplast genomes and microsatellites, there remain gaps between the morphological species concepts proposed by Landrein & Farjon (2020) and the available phylogenetic data. Given that introgression can make phylogenetic reconstruction more difficult, additional nuclear markers such as targeted sequence capture or genotyping-by-sequencing will be useful for testing the roles of introgression and could provide alternative scenarios of the biogeographic diversification of *Diabelia*.

5 Conclusions

Based on 28 complete plastomes (excluding one copy of the IR), a robust phylogenetic framework within *Diabelia* has been established for the first time. Our results showed that *Diabelia* originated in the Japanese archipelago during the Oligocene. Our analyses of the plastome data suggest that the disjunct distribution of *Diabelia ionostachya* var. *wenzhouensis* in China with its closest relative on the islands of Japan could have resulted from a vicariance event. Following divergence, species in China may have experienced a notable in situ extinction of local populations owing to a reduction in suitable habitats during subsequent climatic oscillations. *Diabelia* populations in Japan probably survived in multiple glacial refugia, and *Diabelia* populations that are disjunct between Korea and in the north of Japan may have resulted from a vicariance event. An enhanced understanding of the mechanisms underlying the disjunct distribution of this species in China and Japan requires further studies with increased sample sizes. In the future, we plan to extend the phylogenomic sampling to include large datasets of nuclear genes to fully clarify the timing and processes that have defined species diversity and range evolution in *Diabelia* and its close relatives.

Acknowledgements

We thank Dr. AJ Harris for her advice on biogeographic analyses. This study was funded by the National Natural Science Foundation of China (31660055) and a start-up fund from Hainan University (KYQD1633). The China Scholarship Council (Grant No. 201907565012) supported HFW's research visit to the Smithsonian Institution, Washington, DC, USA.

References

Acosta MC, Premoli AC. 2010. Evidence of chloroplast capture in South American *Nothofagus* (subgenus *Nothofagus*, Nothofagaceae). *Molecular Phylogenetics and Evolution* 54: 235–242.

Allen GA, Soltis DE, Soltis PS. 2003. Phylogeny and biogeography of *Erythronium* (Liliaceae) inferred from chloroplast *matK* and nuclear rDNA ITS sequences. *Systematic Botany* 28: 512–523.

Appelhans MS, Wen J, Duretto M, Crayn D, Wagner WL. 2018. Historical biogeography of *Melicope* (Rutaceae) and its close relatives with a special emphasis on Pacific dispersals. *Journal of Systematics and Evolution* 56: 576–599.

Bai G-Q, Zhou T, Zhao J-X, Li W-M, Han G-J, Li S-F. 2017. The complete chloroplast genome of *Kolkwitzia amabilis* (Caprifoliaceae), an endangered horticultural plant in China. *DNA Sequence* 28: 296–297.

Barrett CF, Baker WJ, Comer JR, Conran JG, Lahmeyer SC, Leebens-Mack JH, Li J, Lim GS, Mayfield-Jones DR, Perez L, Medina J, Chrispires J, Santos C, Stevenson DW, Zomlefer WB, Davis JI. 2016. Plastid genomes reveal support for deep phylogenetic relationships and extensive rate variation among palms and other commelinid monocots. *New Phytologist* 209: 855–870.

Birky CW. 1995. Uniparental inheritance of mitochondrial and chloroplast genes: Mechanisms and evolution. *Proceedings of the National Academy of Sciences USA* 92: 11331–11338.

Burke SV, Grennan CP, Duvall MR. 2012. Plastome sequences of two New World bamboos – *Arundinaria gigantea* and *Cryptochloa strictiflora* (Poaceae) – extend phylogenomic understanding of Bambusoideae. *American Journal of Botany* 99: 1951–1961.

Cao Y-N, Comes HP, Sakaguchi S, Chen L-Y, Qiu Y-X. 2016. Evolution of East Asia's Arcto-Tertiary relict *Euptelea* (Eupteleaceae) shaped by Late Neogene vicariance and Quaternary climate change. *BMC Evolutionary Biology* 16: 1.

Carlquist S. 1996. Plant dispersal and the origin of Pacific island floras. In: Keast A, Miller SE eds. *The origin and evolution of Pacific island biotas, New Guinea to Eastern Polynesia: Patterns and processes*. Amsterdam: SPB Academic Publishing. 153–164.

Chen J-M, Zhao S-Y, Liao Y-Y, Gichira AW, Gituru RW, Wang Q-F. 2015a. Chloroplast DNA phylogeographic analysis reveals significant spatial genetic structure of the relictual tree *Davidia involucrata* (Davidiaceae). *Conservation Genetics* 16: 583–593.

Chen L-Y, Cao Y-N, Yuan N, Koh N, Wang G-M, Qiu Y-X. 2015b. Characterization of transcriptome and development of novel EST-SSR makers based on next-generation sequencing technology in *Neolitsea sericea* (Lauraceae) endemic to East Asian land-bridge islands. *Molecular Breeding* 35: 187.

Choi KS, Chung MG, Park S. 2016. The complete chloroplast genome sequences of three Veroniceae species (Plantaginaceae): Comparative analysis and highly divergent regions. *Trends in Plant Science* 7: 355.

Comes HP, Kadereit JW. 1998. The effect of Quaternary climatic changes on plant distribution and evolution. *Trends in Plant Science* 3: 432–438.

Cox CB, Moore PD. 2005. *Biogeography: An ecological and evolutionary approach*. Oxford: Blackwell Publishing.

Davis MB, Shaw RG. 2001. Range shifts and adaptive responses to Quaternary climate change. *Science* 292: 673–679.

Dick CW, Bermingham E, Lemes MR, Gribel R. 2007. Extreme long-distance dispersal of the lowland tropical rainforest tree *Ceiba pentandra* L. (Malvaceae) in Africa and the Neotropics. *Molecular Ecology* 16: 3039–3049.

Dobson M. 1994. Patterns of distribution in Japanese land mammals. *Mammal Review* 24: 91–111.

Donoghue MJ. 2008. A phylogenetic perspective on the distribution of plant diversity. *Proceedings of the National Academy of Sciences USA* 105: 11549–11555.

Douglas SE. 1998. Plastid evolution: Origins, diversity, trends. *Current Opinion in Genetics & Development* 8: 655–661.

Doyle JA, Sauquet H, Scharaschkin T, Thomas LA. 2004. Phylogeny, molecular and fossil dating, and biogeographic history of Annonaceae and Myristicaceae (Magnoliales). *International Journal of Plant Sciences* 165: S55–S67.

Doyle JJ, Doyle JL. 1987. A rapid DNA isolation procedure for small quantities of fresh leaf tissue. *Phytochemistry* 19: 11–15.

Drummond AJ, Nicholls GK, Rodrigo AG, Solomon W. 2002. Estimating mutation parameters, population history and genealogy simultaneously from temporally spaced sequence data. *Genetics* 16: 1307–1320.

Drummond AJ, Suchard MA, Xie D, Rambaut A. 2012. Bayesian phylogenetics with BEAUti and the BEAST 1.7. *Molecular Biology and Evolution* 29: 1969–1973.

Feng S, Ru DF, Sun Y-S, Mao KS, Miline R, Liu J-Q. 2019. Trans-lineage polymorphism and nonbifurcating diversification of the genus *Picea*. *New Phytologist* 222: 576–587.

Frazer KA, Pachter L, Poliakov A, Rubin EM, Dubchak I. 2004. VISTA: Computational tools for comparative genomics. *Nucleic Acids Research* 32: W273.

Fritsch PW, Manchester SR, Stone RD, Cruz BC, Almeda F, Silman M. 2015. Northern Hemisphere origins of the amphi-Pacific tropical plant family Symplocaceae. *Journal of Biogeography* 42: 891–901.

Gillespie RG, Baldwin BG, Waters JM, Fraser CI, Nikula R, Roderick GK. 2012. Long-distance dispersal: A framework for hypothesis testing. *Trends in Ecology & Evolution* 27: 47–56.

Hahn C, Bachmann L, Chevreux B. 2013. Reconstructing mitochondrial genomes directly from genomic next-generation sequencing reads – A baiting and iterative mapping approach. *Nucleic Acids Research* 41: e129.

Hara H. 1983. A revision of Caprifoliaceae of Japan with reference to allied plants in other districts and the Adoxaceae. *Ginkgoana* 5: 184.

Harris AJ, Ickert-Bond S, Rodríguez A. 2018. Long distance dispersal in the assembly of floras: A review of progress and prospects in North America. *Journal of Systematics and Evolution* 56: 430–448.

Harris AJ, Xiang Q-Y. 2009. Estimating ancestral distributions of lineages with uncertain sister groups – A statistical approach to DIVA and a case using *Aesculus* L. (Sapindaceae) including fossils. *Journal of Systematics and Evolution* 47: 349–368.

Harrison SP, Yu G, Takahara H, Prentice IC. 2001. Palaeovegetation: Diversity of temperate plants in East Asia. *Nature* 413: 129–130.

Hearn DJ, Evans M, Wolf B, McGinty M, Wen J. 2018. Dispersal is associated with morphological innovation, but not increased diversification, in *Cyphostemma* (Vitaceae). *Journal of Systematics and Evolution* 56: 340–359.

Hewitt G. 2000. The genetic legacy of the Quaternary ice ages. *Nature* 405: 907–913.

Hotta M. 1974. *History and geography of plants*. Tokyo: Sanseido.

Huang H, Shi C, Liu Y, Mao S, Gao L. 2014. Thirteen *Camellia* chloroplast genome sequences determinedby high-throughput sequencing: Genome structure and phylogenetic relationships. *BMC Evolutionary Biology* 14: 151.

Huang X-H, Deng T, Moore MJ, Wang H-C, Li Z-M, Lin N, Yusupov Z, Tojibaev KS, Wang Y-H, Sun H. 2019. Tropical Asian origin, boreotropical migration and long-distance dispersal in nettles (Urticeae, Urticaceae). *Molecular Phylogenetics and Evolution* 137: 190–199.

Huelsenbeck JP, Ronquist F. 2001. MrBayes: Bayesian inference of phylogenetic trees. *Bioinformatics* 17: 754–755.

Humphries CJ, Parenti LR. 1986. *Cladistic biogeography*. Oxford: Clarendon Press.

Iijima A, Tada R. 1990. Evolution of Tertiary sedimentary basins of Japan in reference to opening of the Japan Sea. *Journal of the Faculty of Science University of Tokyo* 2: 121–171.

Kamei T, Research Group for the Biogeography from Würm. 1981. Fauna and flora of the Japanese Islands in the last glacial time. *Quaternary Research* 20: 191–205. (in Japanese with English abstract)

Katoh K, Standley DM. 2013. MAFFT multiple sequence alignment software version 7: Improvements in performance and usability. *Molecular Biology and Evolution* 30: 772–780.

Kawabe A, Nukii H, Furihata H. 2018. Exploring the history of chloroplast capture in *Arabis* using whole chloroplast genome sequencing. *International Journal of Molecular Sciences* 19: 602.

Kim JS, Hong JK, Chase MW, Fay MF, Kim JH. 2013. Familial relationships of the monocot order Liliales based on a molecular phylogenetic analysis using four plastid loci: *mat*K, *rbc*L, *atp*B and *atp*F-H. *Biological Journal of the Linnean Society* 172: 5–21.

Krak K, Vít P, Belyayev A, Douda J, Hreusová L, Mandák B. 2016. Allopolyploid origin of *Chenopodium album* s. str. (Chenopodiaceae): A molecular and cytogenetic insight. *PLoS One* 11: e0161063.

Landrein S. 2010. *Diabelia*, a new genus of tribe Linnaeeae subtribe Linnaeinae (Caprifoliaceae). *Phytotaxa* 3: 34–38.

Landrein S, Buerki S, Wang H-F, Clarkson JJ. 2017. Untangling the reticulate history of species complexes and horticultural breeds in *Abelia* (Caprifoliaceae). *Annals of Botany* 120: 257–269.

Landrein S, Farjon A. 2020. A monograph of Caprifoliaceae: Linnaeeae. *Kew Bulletin* 75: 1.

Landrein S, Prenner G, Chase MW, Clarkson JJ. 2012. *Abelia* and relatives: Phylogenetics of Linnaeeae (Dipsacales–Caprifoliaceae s.l.) and a new interpretation of their inflorescence morphology. *Botanical Journal of the Linnean Society* 169: 692–713.

Li E-X, Yi S, Qiu Y-X, Guo J-T, Comes HP, Fu C-X. 2008. Phylogeography of two East Asian species in *Croomia* (Stemonaceae) inferred from chloroplast DNA and ISSR fingerprinting variation. *Molecular Phylogenetics and Evolution* 49: 702–714.

Li S-F, Chang Z-Y, Yuan Y-M. 1996. The origin and dispersal of the genus *Clintonia* Raf. (Liliaceae): Evidence from its cytogeography and morphology. *Caryologia* 49: 125–130.

Liao Y-Y, Gichira AW, Wang Q-F, Chen J-M. 2016. Molecular phylogeography of four endemic *Sagittaria* species (Alismataceae) in the Sino-Japanese Floristic Region of East Asia. *Botanical Journal of the Linnean Society* 180: 6–20.

Librado P, Rozas J. 2009. DnaSP v5: A software for comprehensive analysis of DNA polymorphism data. *Bioinformatics* 25: 1451–1452.

Liu B, Le C-T, Barrett RL, Nickrent DL, Chen Z, Lu L, Vidal-Russell R. 2018. Historical biogeography of Loranthaceae (Santalales): Diversification agrees with emergence of tropical forests and radiation of songbirds. *Molecular Phylogenetics and Evolution* 124: 199–212.

Lohse M, Drechsel O, Kahlau S, Bock R. 2013. OrganellarGenomeDRAW – A suite of tools for generating physical maps of plastid and mitochondrial genomes and visualizing expression data sets. *Nucleic Acids Research* 41: W575–W581.

Lu R-S, Li P, Qiu Y-X. 2017. The complete chloroplast genomes of three *Cardiocrinum* (Liliaceae) species: Comparative genomic and phylogenetic analyses. *Frontiers in Plant Science* 7: 2054.

Ma P-F, Zhang Y-X, Zeng C-X, Guo Z-H, Li D-Z. 2014. Chloroplast phylogenomic analyses resolve deep-level relationships of an intractable bamboo tribe Arundinarieae (Poaceae). *Systems Biology* 63: 933–950.

Maekawa F. 1998. *The origin of plants (Syokubutsuno-kitamichi)*. Tokyo: Yasaka-Syobou.

Manchester SR. 2001. Update on the megafossil flora of Florissant, Colorado. *Denver Museum of Nature and Science* 4: 137.

Martín-Bravo S, Jiménez-Mejías P, Villaverde T, Escudero M, Hahn M, Spalink D, Roalson EH, Hipp AL, the Global Carex Group. 2019. A tale of worldwide success: Behind the scenes of *Carex* (Cyperaceae) biogeography and diversification. *Journal of Systematics and Evolution* 57: 695–718.

Miller MA, Pfeiffer W, Schwartz T. 2010. Creating the CIPRES Science Gateway for inference of large phylogenetic trees. Proceedings of the Gateway Computing Environments Workshop (GCE), New Orleans. 1–8.

Minaya M, Hackel J, Namaganda M, Brochmann C, Vorontsova MS, Besnard G, Catalán P. 2017. Contrasting dispersal histories of broad- and fine-leaved temperate Loliinae grasses: Range expansion, founder events, and the roles of distance and barriers. *Journal of Biogeography* 44: 1980–1993.

Mitsui Y, Chen S-T, Zhou Z-K, Peng C-I, Deng Y-F, Setoguchi H. 2008. Phylogeny and biogeography of the genus *Ainsliaea* (Asteraceae) in the Sino-Japanese region based on nuclear rDNA and plastid DNA sequence data. *Annals of Botany* 101: 111–124.

Nelson G, Platnick NI. 1981. *Systematics and biogeography*. New York: Columbia University Press.

Nie Z-L, Deng T, Meng Y, Sun H, Wen J. 2013. Post-Boreotropical dispersals explain the pantropical disjunction in *Paederia* (Rubiaceae). *Annals of Botany* 111: 873–886.

Nie Z-L, Sun H, Manchester SR, Meng Y, Luke Q, Wen J. 2012. Evolution of the intercontinental disjunctions in six continents in the *Ampelopsis* clade of the grape family (Vitaceae). *BMC Evolutionary Biology* 12: 17.

Niu Y-T, Jabbour F, Barrett RL, Ye J-F, Zhang Z-Z, Lu K-Q, Lu L-M, Chen Z-D. 2018. Combining complete chloroplast genome sequences with target loci data and morphology to resolve species limits in *Triplostegia* (Caprifoliaceae). *Molecular Phylogenetics and Evolution* 129: 15–26.

Nylander JA, Wilgenbusch JC, Warren DL, Swofford DL. 2008. AWTY (are we there yet?): A system for graphical exploration of MCMC convergence in Bayesian phylogenetics. *Bioinformatics* 24: 581–583.

Otero A, Jiménez-Mejías P, Valcárcel V, Vargas P. 2019. Worldwide long-distance dispersal favored by epizoochorous traits in the biogeographic history of Omphalodeae (Boraginaceae). *Journal of Systematics and Evolution* 57: 579–593.

Park M, Park H, Lee H, Lee BH, Lee J. 2018. The complete plastome sequence of an antarctic bryophyte *Sanionia uncinata* (Hedw.) Loeske. *International Journal of Molecular Sciences* 19: 709.

Parks M, Cronn R, Liston A. 2009. Increasing phylogenetic resolution at low taxonomic levels using massively parallel sequencing of chloroplast genomes. *BMC Evolutionary Biology* 7: 84.

Posada D. 2008. jModelTest: Phylogenetic model averaging. *Molecular Biology Evolutionary* 25: 1253–1256.

Price JP, Wagner WL. 2018. Origins of the Hawaiian flora: Phylogenies and biogeography reveal patterns of long-distance dispersal. *Journal of Systematics and Evolution* 56: 600–620.

Qi X-S, Chen C, Hans PC, Sakaguchi S, Liu Y-H, Tanaka N, Sakio H, Qiu Y-X. 2012. Molecular data and ecological niche modelling reveal a highly dynamic evolutionary history of the East Asian Tertiary relict *Cercidiphyllum* (Cercidiphyllaceae). *New Phytologist* 196: 617–630.

Qi X-S, Na Y, Comes HP, Sakaguchi S, Qiu Y-X. 2014. A strong 'filter' effect of the east China Sea land bridge for East Asia's temperate plant species: Inferences from molecular phylogeography and ecological niche modelling of *Platycrater arguta* (Hydrangeaceae). *BMC Evolutionary Biology* 14: 41.

Qian H. 2002. A comparison of the taxonomic richness of temperate plants in East Asia and North America. *American Journal of Botany* 89: 1818–1825.

Qian H, Ricklefs RE. 2000. Large-scale processes and the Asian bias in species diversity of temperate plants. *Nature* 407: 180–182.

Qiu Y-X, Fu C-X, Comes HP. 2011. Plant molecular phylogeography in China and adjacent regions: Tracing the genetic imprints of Quaternary climate and environmental change in the world's most diverse temperate flora. *Molecular Phylogenetics and Evolution* 59: 225–244.

Qiu Y-X, Qi X-S, Jin X-F, Tao X-Y, Fu C-X, Akiyo N, Comes HP. 2009. Population genetic structure, phylogeography,and demographic history of *Platycrater arguta* (Hydrangeaceae) endemic to East China and South Japan inferred from chloroplast DNA sequence variation. *Taxon* 58: 1226–1241.

Raubeson LA, Jansen RK. 2005. Chloroplast genomes of plants. In: Henry RJ ed. *Plant diversity and evolution: Genotypic and phenotypic variation in higher plants*. London: CABI Publishing. 45–68.

Raven PH, Axelrod DI. 1974. Angiosperm biogeography and past continental movements. *Annals of the Missouri Botanical Garden* 61: 539–673.

Ronquist F. 1997. Dispersal-vicariance analysis: A new approach to the quantification of historical biogeography. *Systematic Biology* 46: 195–203.

Sakaguchi S, Horie K, Ishikawa N, Nagano AJ, Yasugi M, Kudoh H, Ito M. 2017. Simultaneous evaluation of the effects of geographic, environmental and temporal isolation in ecotypic populations of *Solidago virgaurea*. *New Phytologist* 216: 1268–1280.

Sakaguchi S, Qiu Y-X, Liu Y-H, Qi X-S, Kim SH, Han J, Takeuchi Y, Worth JR, Yamasaki M, Sakurai S, Isagi Y. 2012. Climate oscillation during the Quaternary associated with landscape heterogeneity promoted allopatric lineage divergence of a temperate tree *Kalopanax septemlobus* (Araliaceae) in East Asia. *Molecular Ecology* 21: 3823–3838.

Santorum JM, Darriba D, Taboada GL, Posada D. 2014. jmodeltest.org: Selection of nucleotide substitution models on the cloud. *Bioinformatics* 30: 1310–1311.

Shin HT, Yi MH, Shin JS, Lee BC, Yoon JW. 2012. Distribution of rare plants – Ulsan, Busan, Yangsan. *Journal of Korean Nature* 5: 145–153.

Stamatakis A. 2014. RAxML version 8: A tool for phylogenetic analysis and post-analysis of large phylogenies. *Bioinformatics* 30: 1312–1313.

Takhtajan A. 1969. *Flowering plants: Origin and dispersal*. Washington, DC: Smithsonian Institution Press.

Takhtajan A. 1986. *Floristic regions of the world*. Berkeley: University of California Press.

Thomas DC, Tang CC, Saunders RMK. 2017. Historical biogeography of *Goniothalamus* and Annonaceae tribe Annoneae: Dispersal-vicariance patterns in tropical Asia and intercontinental tropical disjunctions revisited. *Journal of Biogeography* 44: 2862–2876.

Tian S, Lei S-Q, Hu W, Deng L-L, Li B, Meng Q-L. 2015. Repeated range expansions and inter-/postglacial recolonization routes of *Sargentodoxa cuneata* (Oliv.) Rehd. et Wils. (Lardizabalaceae) in subtropical China revealed by chloroplast phylogeography. *Molecular Phylogenetics and Evolution* 85: 238–246.

Valcárcel V, Wen J. 2019. Chloroplast phylogenomic data support Eocene amphi-Pacific early radiation for the Asian palmate core Araliaceae. *Journal of Systematics and Evolution* 57: 547–560.

Velazco PM, Patterson BD. 2008. Phylogenetics and biogeography of the broad nosed bats, genus *Platyrrhinus* (Chiroptera: Phyllostomidae). *Molecular Phylogenetics and Evolution* 49: 479–489.

Wang H-F, Landrein S, Dong W-P, Nie Z-L, Kondo K, Funamoto T, Wen J, Zhou S-L. 2015. Molecular phylogeny and biogeographic diversification of Linnaeoideae (Caprifoliaceae s.l.) disjunctly distributed in Eurasia, North America and Mexico. *PLoS One* 10: e0116485.

Wang H-X, Liu H, Moore MJ, Landrein S, Liu B, Zhu Z-X, Wang H-F. 2020. Plastid phylogenomic insights into the evolution of the Caprifoliaceae s.l. (Dipsacales). *Molecular Phylogenetics and Evolution* 142: 106641.

Wang J-F, Gong X, Chiang Y-C, Kuroda C. 2013a. Phylogenetic patterns and disjunct distribution in *Ligularia hodgsonii* Hook. (Asteraceae). *Journal of Biogeography* 40: 1741–1754.

Wang Z-H, Peng H, Kilian N. 2013b. Molecular phylogeny of the *Lactuca alliance* (Cichorieae subtribe Lactucinae, Asteraceae) with focus on their Chinese centre of diversity detects potential events of reticulation and chloroplast capture. *PLoS One* 8: e82692.

Wen J. 1999. Evolution of eastern Asian and eastern North American disjunct distributions in flowering plants. *Annual Review of Ecology and Systematics* 30: 421–455.

Wen J, Harris AJ, Kalburgi Y, Zhang N, Xu Y, Zheng W, Ickert-Bond SM, Johnson G, Zimmer EA. 2018. Chloroplast phylogenomics of the New World grape species (*Vitis*, Vitaceae). *Journal of Systematics and Evolution* 56: 297–308.

Wen J, Nie Z-L, Ickert-Bond SM. 2016. Intercontinental disjunctions between eastern Asia and western North America in vascular plants highlight the biogeographic importance of the Bering land bridge from late Cretaceous to Neogene. *Journal of Systematics and Evolution* 54: 469–490.

Wen J, Ree RH, Ickert-Bond S, Nie Z-L, Funk VA. 2013. Biogeography: Where do we go from here? *Taxon* 62: 912–927.

Wiley EO. 1980. Phylogenetic systematics and vicariance biogeography. *Systems Biology* 5: 194–220.

Wolfe KH, Li W-H, Sharp PM. 1987. Rates of nucleotide substitution vary greatly among plant mitochondrial, chloroplast, and nuclear DNAs. *Proceedings of the National Academy of Sciences USA* 84: 9054–9058.

Wyman SK, Jansen RK, Boore JL. 2004. Automatic annotation of organellar genomes with DOGMA. *Bioinformatics* 20: 3252–3255.

Xi Z, Ruhfel BR, Schaefe H, Amorim AM, Sugumaran M, Wurdack KJ, Endress PK, Matthews ML, Stevens PF, Mathews S. 2012. Phylogenomics and a posteriori data partitioning resolve the Cretaceous angiosperm radiation. *Proceedings of the National Academy of Sciences USA* 109: 17519–17524.

Xiang Q-Y, Soltis DE. 2001. Dispersal-vicariance analyses of intercontinental disjuncts: Historical biogeographical implications for angiosperms in the Northern Hemisphere. *International Journal of Plasticity* 162 (Suppl.): S29–S39.

Yang Q, Landrein S. 2011. Linnaeaceae. In: Wu ZY, Raven PH, Hong DY eds. *Flora of China*. Beijing: Science Press; St. Louis: Missoui Botanical Garden Press. 19: 642–648.

Yang T, Lu L-M, Wang W, Li J-H, Manchester SR, Wen J, Chen Z-D. 2018. Boreotropical range expansion and long-distance dispersal explain two amphi-Pacific tropical disjunctions in sabiaceae. *Molecular Phylogenetics and Evolution* 124: 181–191.

Yi T-S, Jin G-H, Wen J. 2015. Chloroplast capture and intra- and inter-continental biogeographic diversification in the Asian–New World disjunct plant genus *Osmorhiza* (Apiaceae). *Molecular Phylogenetics and Evolution* 85: 10–21.

Yoder AD, Nowak MD. 2006. Has vicariance or dispersal been the predominant biogeographic force in Madagascar? Only time will tell. *The Annual Review of Ecology, Evolution, and Sytematics* 37: 405–431.

Yu G, Chen X, Ni J, Cheddadi R, Guiot J, Han H, Harrison SP, Huang C, Ke M, Kong Z, Li S, Li W, Liew P, Liu G, Liu J, Liu Q, Liu K-B, Prentice IC, Qui W, Ren G, Song C, Sugita S, Sun X, Tang L, Van Campo E, Xia Y, Xu Q, Yan S, Yang X, Zhao J, Zheng Z. 2000. Palaeovegetation of China: A pollen data-based synthesis for the mid-Holocene and last glacial maximum. *Journal of Biogeography* 27: 635–664.

Yu Y, Blair C, He XJ. 2019. RASP (Reconstruct Ancestral State in Phylogenies): A tool for historical biogeography. *Molecular Biology and Evolution.* doi: 10.1093/molbev/msz257.

Yu Y, Harris AJ, Blair C, He XJ. 2015. RASP (Reconstruct Ancestral State in Phylogenies): A tool for historical biogeography. *Molecular Phylogenetics and Evolution* 87: 46–49.

Yu Y, Harris AJ, He X-J. 2010. S-DIVA (Statistical Dispersal-Vicariance Analysis): A tool for inferring biogeographic histories. *Molecular Phylogenetics and Evolution* 56: 848–850.

Yuan Y-W, Olmstead RG. 2008. A species-level phylogenetic study of the *Verbena* complex (Verbenaceae) indicates two independent intergeneric chloroplast transfers. *Molecular Phylogenetics and Evolution* 48: 23–33.

Zachos J, Pagani M, Sloan L, Thomas E, Billups K. 2001. Trends, rhythms, and aberrations in global climate 65 Ma to present. *Science* 292: 686–693.

Zhai S-N, Comes PH, Nakamura K, Yan H-F, Qiu Y-X. 2012. Late Pleistocene lineage divergence among populations of *Neolitsea sericea* (Lauraceae) across a deep sea-barrier in the Ryukyu Islands. *Journal of Biogeography* 39: 1347–1360.

Zhang X, Zhang H-J, Landis JB, Deng T, Meng A-P, Sun H, Peng Y-S, Wang H-C, Sun Y-X. 2019. Plastome phylogenomic analysis of *Torreya* (Taxaceae). *Journal of Systematics and Evolution* 57: 607–615.

Zhao K-K, Landrein S, Barrett RL, Sakaguch S, Maki M, Mu W-X, Yang T, Zhu Z-X, Liu H, Wang H-F. 2019. Phylogeographic analysis and genetic structure of an endemic Sino-Japanese disjunctive genus *Diabelia* (Caprifoliaceae). *Frontiers in Plant Science* 10: 913.

Zhao L, Potter D, Xu Y, Liu P-L, Johnson G, Chang Z-Y, Wen J. 2018. Phylogeny and spatio-temporal diversification of *Prunus* subgenus *Laurocerasus* section *Mesopygeum* (Rosaceae) in the Malesian region. *Journal of Systematics and Evolution* 56: 637–651.

Zhou S-L, Wen J. 2006. Discovery of *Abelia spathulata* (Caprifoliaceae) in eastern China. *Acta Phytotaxonomica Sinica* 44: 467–470.

Appendix 1

The name *Abelia ionostachya* Nakai was recognised as having nomenclatural priority (when recognised at species rank) over *Abelia spathulata* Siebold & Zucc. var. *stenophylla* Honda shortly prior to the publication of Landrein & Farjon (2020). However, page proofs had already been approved and the change could not be made in that paper, so we make the necessary nomenclatural combinations here. Full synonymy for each taxon is presented in Landrein & Farjon (2020).

Diabelia ionostachya (Nakai) Landrein & R. L. Barrett, *comb. nov*.

Basionym: *Abelia ionostachya* Nakai, *Bull. Natl. Sci. Mus., Tokyo* 33: 23 (1953). *Type*: Honshu, Niigata, Kirinzan, Tsugawa-machi, 26 May 1950, *T. Nakai* & *N. Maruyama s.n.* (holotype TNS 83706!).

Abelia spathulata Siebold & Zucc. var. *stenophylla* Honda, *Bot. Mag.* (*Tokyo*) 50: 436 (1936); *Diabelia stenophylla* (Honda) Landrein in Landrein & Farjon, *Kew Bull.*, 75:1: 183 (2020). *Type*: Japan, Honshu, Akita, Higashidatemura, Kitaakita-gun, June 1931, *M. Matsuda* 14b (holotype TI!), *syn. nov*.

Diabelia ionostachya (Nakai) Landrein & R. L. Barrett var. ***ionostachya***

Diabelia ionostachya (Nakai) Landrein & R. L. Barrett var. ***tetrasepala*** (Koidz.) Landrein, *comb. nov*.

Basionym: *Abelia spathulata* Siebold & Zucc. var. *tetrasepala* Koidz., *Bot. Mag.* (*Tokyo*) 29(348): 311 (1915); *Abelia tetrasepala* (Koidz.) H.Hara & S. Kuros. in Kurosawa & Hara, *J. Jap. Sci.* 30: 296 (1955); *Diabelia tetrasepala* (Koidz.) Landrein, *Phytotaxa* 3: 37 (2010). *Diabelia stenophylla* (Honda) Landrein var. *tetrasepala* (Koidz.) Landrein in Landrein & Farjon, *Kew Bull.*, 75:1: 186 (2020). *Type*: Japan, Honshu, Saitama Pref. [Musashi, Chichibu], 23 April 1878, *J. Matsumara s.n.* (holotype TI!).

Diabelia ionostachya (Nakai) Landrein & R. L. Barrett var. ***wenzhouensis*** (S. L. Zhou ex Landrein) Landrein, *comb. nov*.

Basionym: *Diabelia stenophylla* (Honda) Landrein var. *wenzhouensis* S. L. Zhou ex Landrein in Landrein & Farjon, *Kew Bull.*, 75:1: 189 (2020). *Type*: China, Zhejiang, Wenzhou Pref., Yongjia Xian, Sihai Mts, 20 May 2002, *S. L. Zhou* & *S. T. Lu 2002520* (holotype PE!).

Supplementary Material

The following supplementary material is available online for this article at http://onlinelibrary.wiley.com/doi/10.1111/jse.12560/suppinfo:

Fig. S1. (**A**) Map of *Diabelia* plastomes. Genes shown on the outside of the circle are transcribed clockwise, and genes inside are transcribed counter-clockwise. Genes belonging to different functional groups are color-coded. The darker gray in the inner corresponds to the GC content, and the lighter gray to the AT content. (**B**) mVISTA-based identity plots among all available plastomes of *Diabelia*. Gray arrows above the alignment indicate genes and their orientation. A cut-off of 70% identity was used for the plots. The Y axis indicates the percent identity (50–100%) and the X axis indicates the coordinates within the plastome. Genome regions are color-coded as protein coding, rRNA coding, tRNA coding or conserved non-coding sequences. The red solid lines show the inverted repeats (IRs) in the plastomes. (**C**) Comparison of nucleotide diversity (*Pi*) values in 28 individuals within *Diabelia*. (A) Coding regions and (B) Non-coding regions. Refer to Table S1 for detailed data in this figure.

Fig. S2. (**I**) Bayesian inference (BI) and Maximum likelihood (ML) phylogram of *Diabelia* based on LSC regions, with ambiguous sites excluded from analysis. Numbers associated with branches are ML bootstrap values and Bayesian posterior probabilities, respectively. Asterisks indicate 100% bootstrap support or 1.0 posterior probability whereas hyphens indicate the bootstrap support or posterior probability <50% or 0.5. Clade designations are described in the text. (**II**) Bayesian inference (BI) and Maximum likelihood (ML) phylogram of *Diabelia* based on SSC regions, with ambiguous sites excluded from analysis. Numbers associated with branches are ML bootstrap values and Bayesian posterior probabilities, respectively. Asterisks indicate 100% bootstrap support or 1.0 posterior probability whereas hyphens indicate the bootstrap support or posterior probability <50% or 0.5. Clade designations are described in the text. (**III**) Bayesian inference (BI) and Maximum likelihood (ML) phylogram of *Diabelia* based on IR regions, with ambiguous sites excluded from analysis. Numbers associated with branches are ML bootstrap values and Bayesian posterior probabilities, respectively. Asterisks indicate 100% bootstrap support or 1.0 posterior probability whereas hyphens indicate the bootstrap support or posterior probability <50% or 0.5. Clade designations are described in the text. (**IV**) Bayesian inference (BI) and Maximum likelihood (ML) phylogram of *Diabelia* based on complete plastome sequences, with ambiguous sites excluded from analysis. Numbers associated with branches are ML bootstrap values and Bayesian posterior probabilities, respectively. Asterisks indicate 100% bootstrap support or 1.0 posterior probability whereas hyphens indicate the bootstrap support or posterior probability <50% or 0.5. Clade designations are described in the text. (**V**) Bayesian inference (BI) and Maximum likelihood (ML) phylogram of *Diabelia* based on plastome coding regions, with ambiguous sites excluded from analysis. Numbers associated with branches are ML bootstrap values and Bayesian posterior probabilities, respectively. Asterisks indicate 100% bootstrap support or 1.0 posterior probability whereas hyphens indicate the bootstrap support or posterior probability <50% or 0.5. Clade designations are described in the text. (**VI**) Bayesian inference (BI) and Maximum likelihood (ML) phylogram of *Diabelia* based on plastome noncoding regions, with ambiguous sites excluded from analysis. Numbers associated with branches are ML bootstrap values and Bayesian posterior probabilities, respectively. Asterisks indicate 100% bootstrap support or 1.0 posterior probability whereas hyphens indicate the bootstrap support or posterior probability <50% or 0.5. Clade designations are described in the text.

Table S1. (**I**) Overview of the plastome data for the 28 individuals of *Diabelia* species used for divergence analysis. (**II**) Data set characteristics, including models selected in maximum likelihood (ML) and Bayesian inference (BI) analyses for each dataset, as well as relationships among *Diabelia* obtained from different analyses.